

Supplementary Information

Optimized Electronic Properties and nano-Structural Features for Securing High Thermoelectric Performance in Doped GeTe

Zan Yang ^a, Yu-Chih Tseng ^b, Suneesh Meledath Valiyaveettil ^{c, d}, Hui Yuan ^e, Evan Smith ^f,
Kuei-Hsien Chen ^{c, d}, Yuyang Huang ^a, Tianze Zou ^g, Jan Kycia ^g and Yurij Mozharivskyj*^a

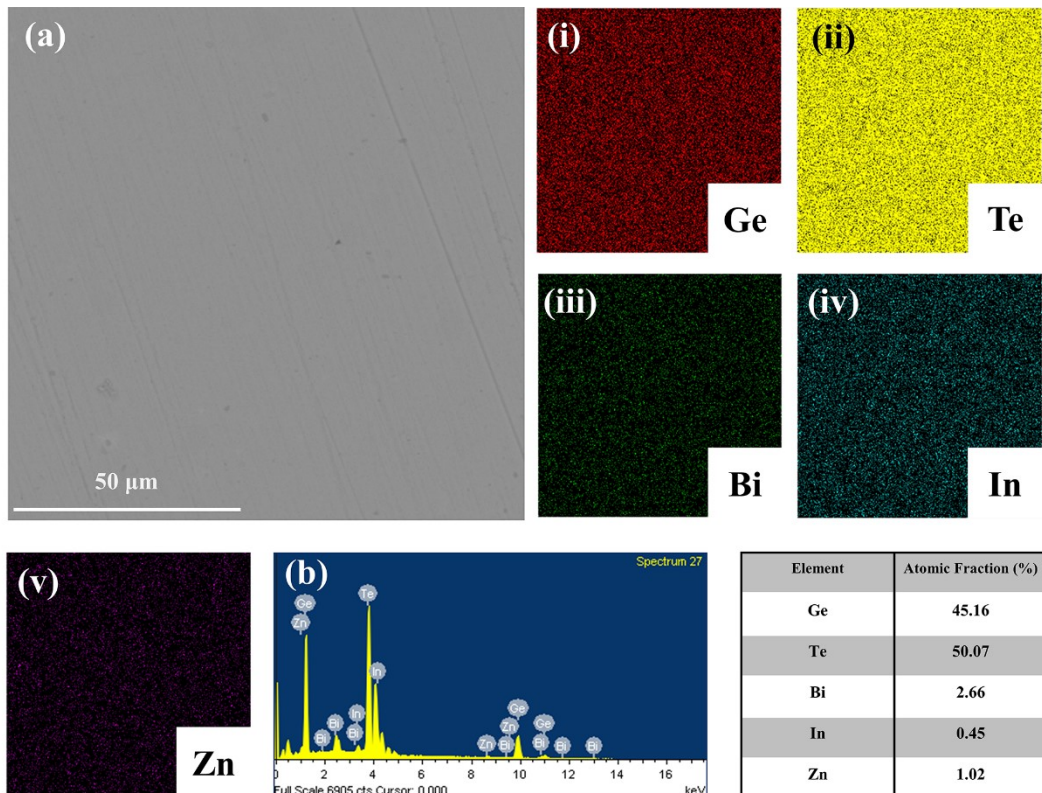


Figure S1. SEM images of $(\text{Ge}_{0.97}\text{Zn}_{0.02}\text{In}_{0.01}\text{Te})_{0.97}(\text{Bi}_2\text{Te}_3)_{0.03}$. (a) Back scattered electron (BSE) image, (b) energy dispersive spectroscopy (EDS) spectrum and the corresponding elemental concentrations, (i) ~ (v) elemental mappings.

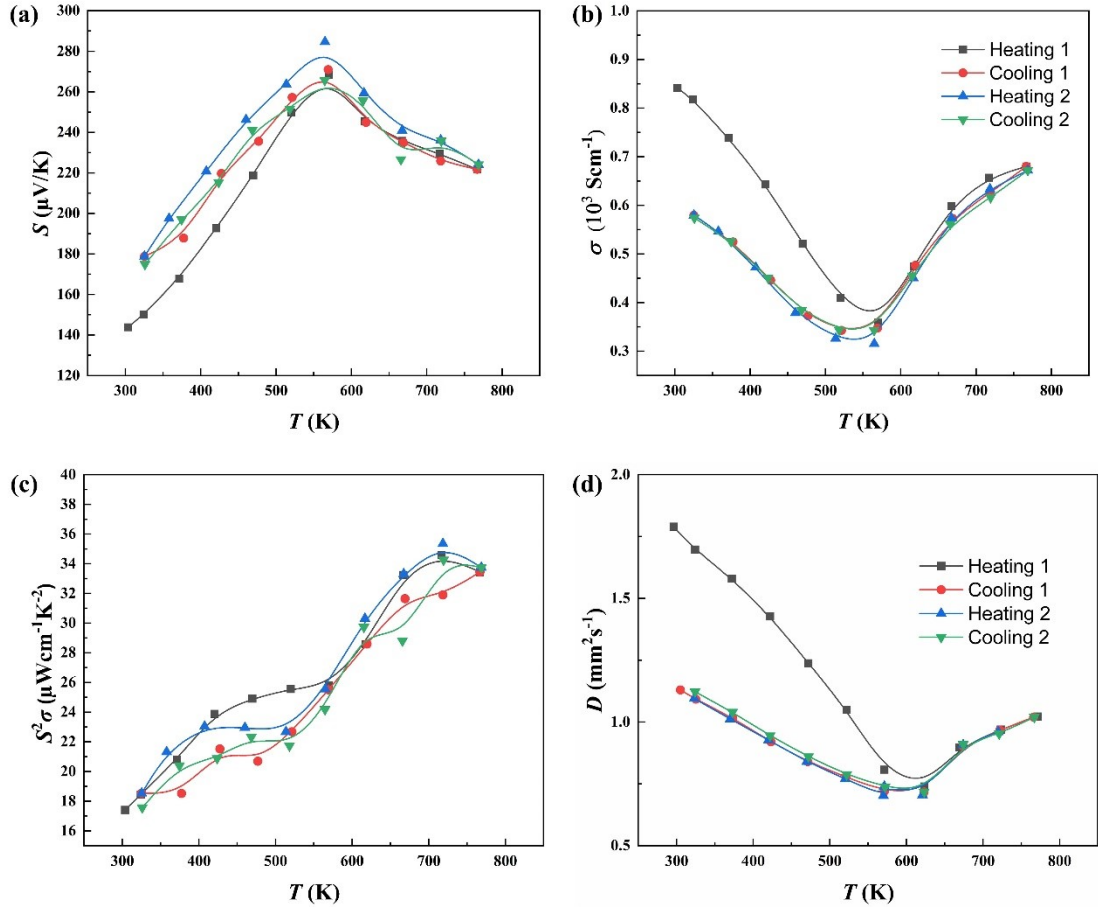


Figure S2. ZEM thermal loop of $\text{Ge}_{0.95}\text{Bi}_{0.05}\text{Te}$. (a) Seebeck coefficient, (b) electrical resistivity, (c) power factor, (d) thermal diffusivity.

Single Kane Band Model

Since GeTe is a narrow band gap semiconductor, the strong interactions between the conduction and valence bands makes the non-parabolicity at the valence band maximum impossible to be ignored. Therefore, a Single-Kane Band (SKB) model was developed to calculate the Lorenz number and DOS effective mass based on Pei et al.'s work². The expressions for the transport coefficients are as follow:

Seebeck coefficient S

$$S = \frac{k_B}{e} \left[\frac{^1F_{-2}^1}{^0F_{-2}^1} - \xi \right] \quad (\text{S1})$$

Lorenz number L

$$L = \left(\frac{k_B}{e}\right)_2^2 \left[\frac{{}^2F_{-2}^1}{{}^0F_{-2}^1} - \left(\frac{{}^1F_{-2}^1}{{}^0F_{-2}^1}\right)_2^2 \right] \quad (\text{S2})$$

Single band effective mass m_b^*

$$m_b^* = \frac{1}{2k_B T} \left[\frac{3Ap_H\pi^2\hbar^3}{N_V} \left({}^0F_0^{3/2}\right)^{-1} \right]^{2/3} \quad (\text{S3})$$

Hall factor A

$$A = \frac{3K(K+2) {}^0F_{-4}^{1/2} {}^0F_0^{3/2}}{(2K+1)^2 \left({}^0F_{-2}^1\right)^2} \quad (\text{S4})$$

Where ${}^nF_k^m$ is the α included Fermi integral

$${}^nF_k^m = \int_0^\infty \left(-\frac{\partial f}{\partial \varepsilon} \right) \varepsilon^n (\varepsilon + \alpha \varepsilon^2)^m [(1 + 2\alpha\varepsilon)^2 + 2]^{k/2} d\varepsilon \quad (\text{S5})$$

ε ($\varepsilon = E / k_B T$) is the reduced energy, f is the Fermi-Dirac distribution, α ($\alpha = k_B T / E_g$)

is the non-parabolic parameter, E_g is the band gap, ξ ($\xi = E_f / k_B T$) is the reduced Fermi

level, N_v is the band degeneracy, $K = m_{//}^* / m_{\perp}^*$ is the anisotropy factor. For GeTe, $K = 2^3$. The SKB model is solved by the Python code and the flow chart of its basic logic is shown in below.

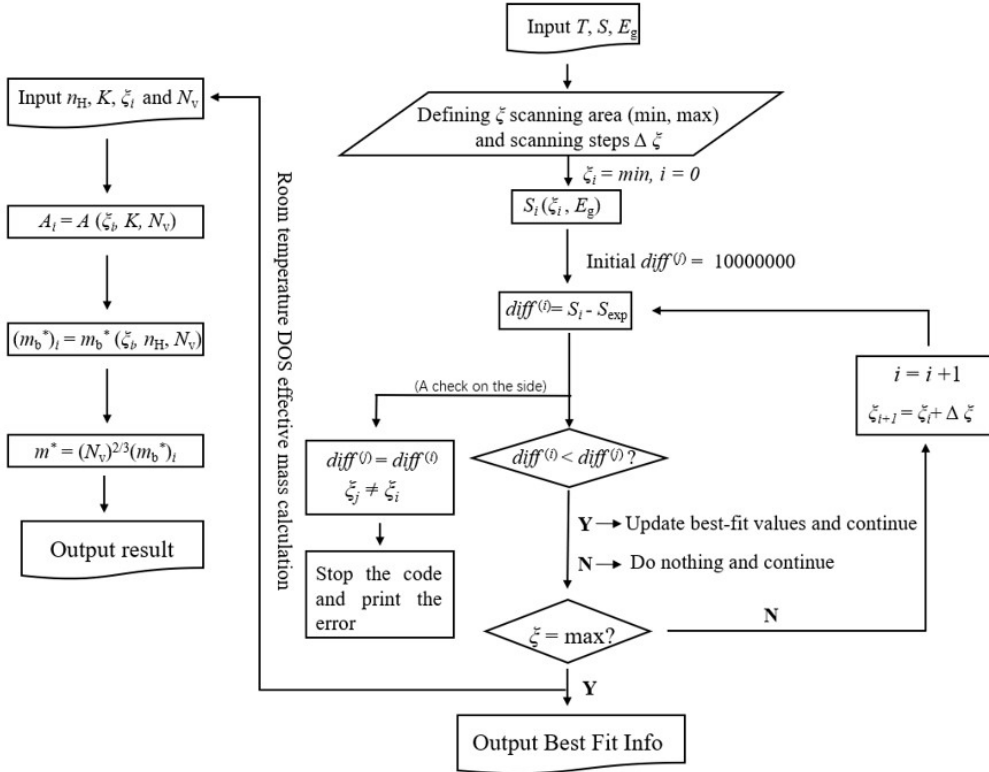


Figure S3. (a) Basic logic of the SKB solving code. (b) Carrier concentration obtained by the Hall effect measurements. (c) DOS effective mass calculated by the SKB model. The exact value of both (b) and (c) could be found in **Table S4**. Here, y is the doping level of Zn.

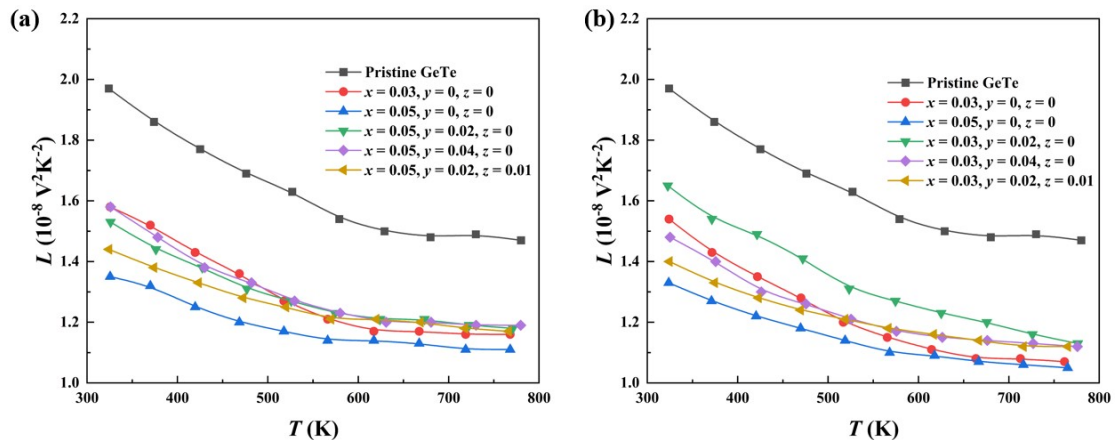


Figure S4. Lorenz number of (a) NCB and (b) CB, respectively.

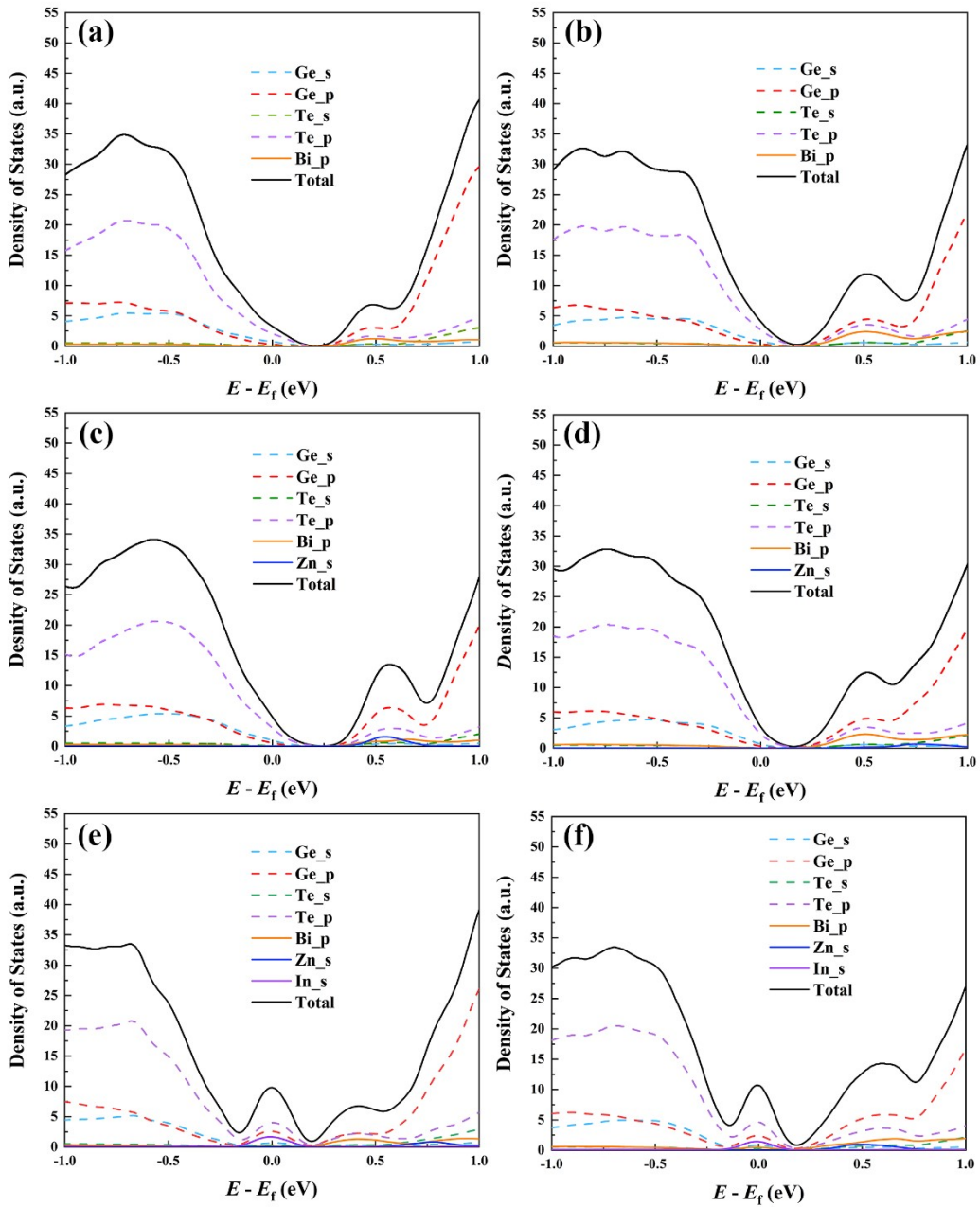


Figure S5. Partial density of states of (a) $\text{Ge}_{26}\text{BiTe}_{27}$, (b) $\text{Ge}_{24}\text{Bi}_2\text{Te}_{27}$, (c) $\text{Ge}_{25}\text{BiZnTe}_{27}$, (d) $\text{Ge}_{23}\text{Bi}_2\text{ZnTe}_{27}$, (e) $\text{Ge}_{24}\text{BiZnInTe}_{27}$ and (f) $\text{Ge}_{22}\text{Bi}_2\text{ZnInTe}_{27}$. (a), (c), (d) belongs to the NCB system; (b), (d), (f) belongs to the CB system. The Fermi energy is determined from the Hall carrier concentration.

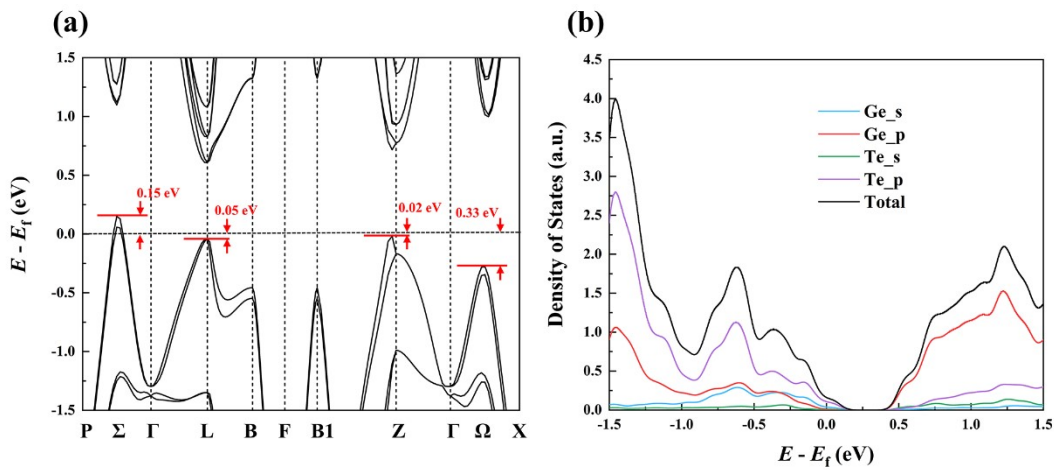


Figure S6. (a) Band structure and (b) partial density of state of GeTe.

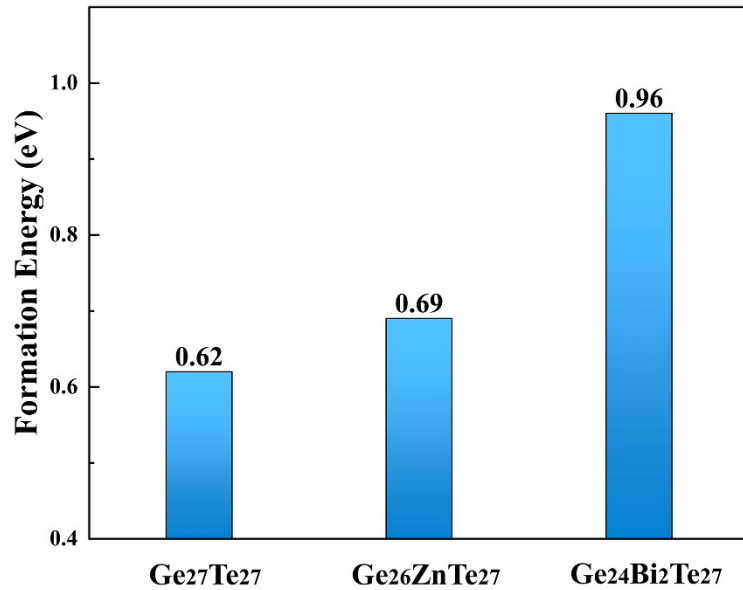


Figure S7. Formation energy of a Ge vacancy defect, calculated for Ge₂₇Te₂₇, Ge₂₆ZnTe₂₇ and Ge₂₄Bi₂Te₂₇.

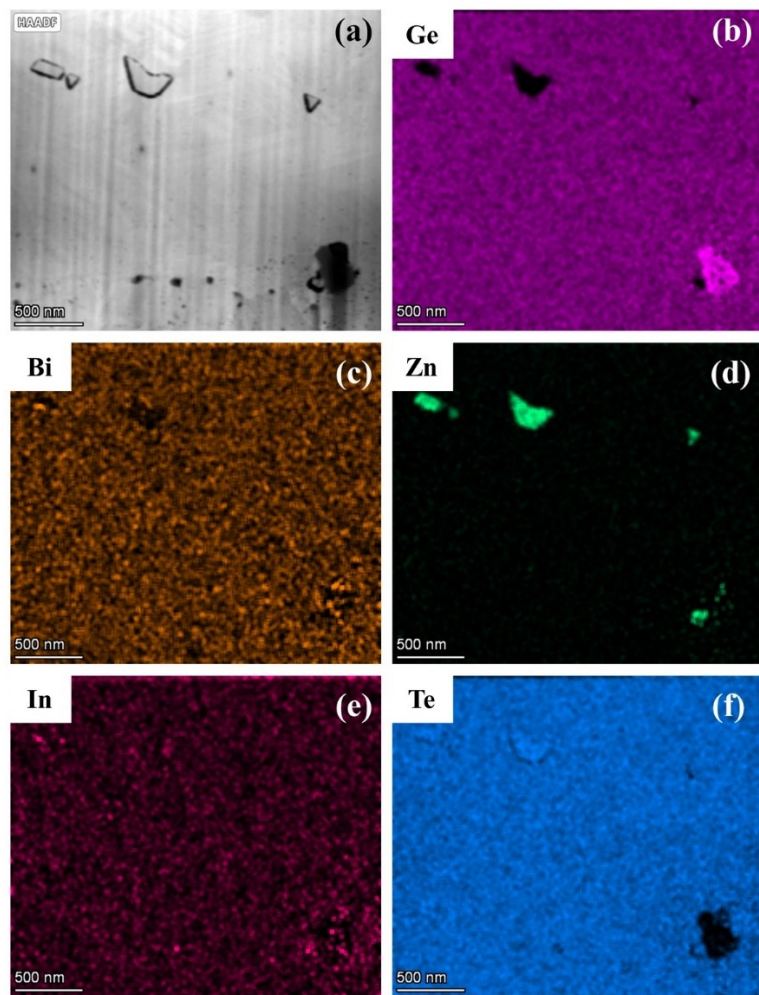


Figure S8. (a) STEM image of $(\text{Ge}_{0.97}\text{Zn}_{0.02}\text{In}_{0.01}\text{Te})_{0.97}(\text{Bi}_2\text{Te}_3)_{0.03}$. This image belongs to another Plasma-FIB lifted sample from the same sample. (b) ~ (f) EDS mapping of Ge, Bi, Zn, In, and Te, respectively. The gray particles are ZnTe precipitations and the black particle at the lower right corner is a Ge precipitation.

Table S1. Experimental densities, theoretical densities, and the corresponding relative densities.

<i>x/y/z</i>	Experimental Density (g/cm ³)	Theoretical Density (g/cm ³)	Relative Density (%)
Pristine GeTe	6.03	6.14	98.17
Ge_{1-x}Bi_xZn_yIn_zTe -- NCB			
0.03/0/0	6.11	6.26	97.60
0.05/0/0	6.10	6.35	96.06
0.05/0.02/0	6.11	6.34	96.37
0.05/0.04/0	6.06	6.34	95.58
0.05/0.02/0.01	6.06	6.35	95.43
(Ge_{1-y-z}Zn_yIn_zTe)_{1-x}(Bi₂Te₃)_x -- CB			
0.03/0/0	6.06	6.31	96.04
0.05/0/0	6.34	6.42	98.75
0.03/0.02/0	6.28	6.31	99.52
0.03/0.04/0	6.10	6.30	96.82
0.03/0.02/0.01	6.06	6.32	95.89

Table S2. Cell parameters extracted from the Rietveld refinement.

$x/y/z$	a (Å)	c (Å)	c/a	Ω (Å ³)
Pristine GeTe	4.1660(6)	10.669(2)	2.56	160.36(5)
$\text{Ge}_{1-x}\text{Bi}_x\text{Zn}_y\text{In}_z\text{Te}$ -- NCB				
0.03/0/0	4.18114(9)	10.643(3)	2.54	161.14(6)
0.05/0/0	4.18999(5)	10.625(1)	2.53	161.54(1)
0.05/0.02/0	4.19689(5)	10.600(1)	2.53	161.70(1)
0.05/0.04/0	4.19640(7)	10.605(1)	2.53	161.73(2)
0.05/0.02/0.01	4.19969(5)	10.582(1)	2.52	161.64(1)
$(\text{Ge}_{1-y-z}\text{Zn}_y\text{In}_z\text{Te})_{1-x}(\text{Bi}_2\text{Te}_3)_x$ -- CB				
0.03/0/0	4.19240(2)	10.6152(7)	2.53	161.58(6)
0.05/0/0	4.21100(2)	10.5531(5)	2.51	162.06(8)
0.03/0.02/0	4.19223(3)	10.6004(8)	2.53	161.34(1)
0.03/0.04/0	4.20088(2)	10.5965(5)	2.52	161.95(1)
0.03/0.02/0.01	4.20200(2)	10.5799(5)	2.52	161.780 (8)

Table S3. Hall measurement data.

$x/y/z$	μ_H (cm ² /V·s)	p_H (10 ²⁰ cm ⁻³)	m^* (m_e)
Pristine GeTe	81.8	5.17	1.88
$\text{Ge}_{1-x}\text{Bi}_x\text{Zn}_y\text{In}_z\text{Te}$ -- NCB			
0.03/0/0	71.4	3.22	2.23
0.05/0/0	34.6	1.75	3.71
0.05/0.02/0	73.0	0.81	1.28
0.05/0.04/0	60.6	0.85	1.12
0.05/0.02/0.01	24.9	2.16	3.58
$(\text{Ge}_{1-y-z}\text{Zn}_y\text{In}_z\text{Te})_{1-x}(\text{Bi}_2\text{Te}_3)_x$ -- CB			
0.03/0/0	36.5	3.51	2.29
0.05/0/0	20.5	2.09	3.37
0.03/0.02/0	51.3	2.22	1.51
0.03/0.04/0	61.1	0.80	1.24
0.03/0.02/0.01	23.7	2.28	3.37

* The density of state effective mass is calculated by the developed single Kane band model and is in the unit of free electron mass m_e .

References

- (1) Snyder, G. J.; Snyder, A. H.; Wood, M.; Gurunathan, R.; Snyder, B. H.; Niu, C. Weighted Mobility. *Adv. Mater.* **2020**, *32* (25), 2001537. <https://doi.org/10.1002/adma.202001537>.
- (2) Pei, Y.; LaLonde, A. D.; Wang, H.; Snyder, G. J. Low Effective Mass Leading to High Thermoelectric Performance. *Energy Environ. Sci.* **2012**, *5* (7), 7963. <https://doi.org/10.1039/c2ee21536e>.
- (3) Madelung, O.; Rössler, U.; Schulz, M. General Introduction: Datasheet from Landolt-Börnstein - Group III Condensed Matter · Volume 41C: “Non-Tetrahedrally Bonded Elements and Binary Compounds I” in SpringerMaterials ([Https://Doi.Org/10.1007/10681727_1](https://doi.org/10.1007/10681727_1)). https://doi.org/10.1007/10681727_1.